Available online at www.sciencedirect.com
ScienceDirect
International Journal of Heat and Fluid Flow 28 (2007) 268–274
International Journal of HEAT AND FLUID FLOW
www.elsevier.com/locate/ijhff

Large eddy simulation of scalar turbulence using a new subgrid eddy diffusivity model

Yu Guo [a], Chun-Xiao Xu [a,*], Guixiang Cui [a], Zhaoshun Zhang [a], Liang Shao [b]

[a] *Department of Engineering Mechanics, Tsinghua University, Beijing 100084, PR China*
[b] *Laboratory of Fluid Mechanics and Acoustics, Ecole Centrale de Lyon, France*

Received 16 December 2004; received in revised form 6 April 2006; accepted 14 April 2006
Available online 27 June 2006

Abstract

A new subgrid eddy diffusivity model is used for large eddy simulation of scalar turbulence. The new model is based on the modified Yaglom equation, i.e., the dynamical equation for the structure function of resolved-scale scalar fluctuations, by which the scalar transport between resolved grid scale and unresolved subgrid scale can be described exactly. The new model has been applied in the large eddy simulations of scalar transport in both decaying isotropic turbulence and fully developed turbulent channel flow. By the comparison with Smagorinsky model and the dynamical model, it is found that the new model can achieve similar accuracy as the dynamical model, and can reduce the computational cost about 20% in terms of CPU time relative to the dynamical model.

Keywords: Large eddy simulation; Scalar turbulence; Subgrid eddy diffusivity model

1. Introduction

Large eddy simulation (LES) has been considered as the most hopeful candidate to numerically predict complex engineering turbulent flows with sufficient accuracy in the foreseeable future. A key issue in LES is the subgrid scale (SGS) models.

For velocity turbulence, there are several types of SGS models that are used frequently in LES such as the Smagorinsky model, scale-similarity model and dynamical model. In the prediction of complex turbulent flows, the accuracy and the efficiency of these models are still not satisfactory. Recently, Cui et al. (2004) proposed a new subgrid eddy viscosity model based on the modified Kolmogorov equation, i.e., the dynamical equation for the structure function of resolved-scale velocity fluctuations, by which the energy transfer between resolved scale and unresolved subgrid scale can be described exactly.

For the large eddy simulation of scalar turbulence, an analogy is often made between the modelling of subgrid scalar flux and the subgrid modelling of the turbulent velocity field. It is the easy way to obtain the eddy diffusivity coefficient from the eddy viscosity coefficient by an assumption regarding the subgrid Prandtl or Schmit number. But scalar turbulence has its own speciality that is not possessed by velocity turbulence, and more and more researchers find that it is not rational to determine the eddy diffusivity by the simple analogy to eddy viscosity through a subgrid Prandtl number (Lesieur and Rogallo, 1989; Bogucki et al., 1997; Mydlarski and Warhaft, 1998; Zhou et al., 2002). It is necessary to establish the SGS model for scalar turbulence according to its own dynamical properties.

We have noticed that Cui et al. (2004) proposed a rational way to construct the subgrid eddy viscosity model, which is derived from the modified Kolmogorov equation. The Yaglom equation plays a similar role in scalar turbulence as that of the Kolmogorov equation in velocity turbulence. It is suggested that the rational subgrid eddy diffusivity can be formulated using the modified Yaglom

* Corresponding author. Tel.: +86 10 6278 5551; fax: +86 10 6278 1824.
E-mail address: xucx@tsinghua.edu.cn (C.-X. Xu).

0142-727X/$ - see front matter © 2006 Elsevier Inc. All rights reserved.
doi:10.1016/j.ijheatfluidflow.2006.04.003

equation, i.e., the dynamical equation for the structure function of the resolved-scale scalar fluctuations. Using the modified Yaglom equation, the scalar transport between resolved grid scale and unresolved subgrid scale can be exactly taken into consideration.

In the following, the formulation of the new eddy diffusivity model will be shown in Section 2. In Section 3, the new model will be evaluated by the application in LES of scalar transport in decaying isotropic turbulence and in fully developed turbulent channel flow. Conclusions and further discussions will be given in Section 4.

2. Formulation of the new subgrid eddy diffusivity model

At high Reynolds number and Peclet number, velocity and scalar turbulence can be assumed locally isotropic. The dynamics of structure function for local isotropic scalar turbulence is governed by Yaglom equation. If the local isotropy is assumed still valid for resolved scale scalar fluctuations in large eddy simulation, the dynamical equation for the structure function of resolved scale scalar fluctuations can be obtained by analogy with the derivation of Yaglom equation, and the new model for subgrid eddy diffusivity can be formulated.

2.1. Dynamical equation for the structure function of resolved-scale scalar fluctuation

To derive the dynamical equation for the structure function of the resolved-scale scalar fluctuations, we start from the filtered scalar transport equation

$$\frac{\partial\bar{\theta}}{\partial t}+\bar{u}_j\frac{\partial\bar{\theta}}{\partial x_j}=\kappa\frac{\partial^2\bar{\theta}}{\partial x_j\partial x_j}+\frac{\partial\tau_{\theta j}}{\partial x_j}, \tag{1}$$

in which $\tau_{\theta j}=-(\overline{\theta u_j}-\bar{\theta}\bar{u}_j)$, represents the subgrid flux of scalar that should be modelled to close the equation. The overbar denotes the filtering of turbulent quantities such as

$$\bar{\theta}=\int\theta(\mathbf{x}',t)G(\mathbf{x}-\mathbf{x}')\,\mathrm{d}\mathbf{x}'. \tag{2}$$

Eq. (1) can be written at ($\mathbf{x}'$, t) as

$$\frac{\partial\bar{\theta}'}{\partial t}+\bar{u}'_j\frac{\partial\bar{\theta}'}{\partial x'_j}=\kappa\frac{\partial^2\bar{\theta}'}{\partial x'_j\partial x'_j}+\frac{\partial\tau'_{\theta j}}{\partial x'_j}, \tag{3}$$

in which the superscript $'$ denotes the flow quantities at $\mathbf{x}'$, i.e., $\bar{\theta}'=\bar{\theta}(\mathbf{x}',t)$. Subtracting Eq. (1) from (3), we obtain the equation for scalar difference

$$\begin{aligned}&\frac{\partial(\bar{\theta}'-\bar{\theta})}{\partial t}+\bar{u}'_j\frac{\partial\bar{\theta}'}{\partial x'_j}-\bar{u}_j\frac{\partial\bar{\theta}}{\partial x_j}\\&\quad=\kappa\frac{\partial^2\bar{\theta}'}{\partial x'_j\partial x'_j}-\kappa\frac{\partial^2\bar{\theta}}{\partial x_j\partial x_j}+\frac{\partial\tau'_{\theta j}}{\partial x'_j}-\frac{\partial\tau_{\theta j}}{\partial x_j}.\end{aligned} \tag{4}$$

Define $\delta\bar{\theta}=\bar{\theta}'-\bar{\theta}$ to represent the difference of the filtered scalar at $\mathbf{x}'$ and $\mathbf{x}$, and we have

$$\frac{\partial\bar{\theta}'}{\partial x'_j}=\frac{\partial\delta\bar{\theta}}{\partial x'_j},\quad \frac{\partial\bar{\theta}}{\partial x_j}=-\frac{\partial\delta\bar{\theta}}{\partial x_j}. \tag{5}$$

Considering the above relations, Eq. (4) becomes

$$\frac{\partial\delta\bar{\theta}}{\partial t}+\bar{u}'_j\frac{\partial\delta\bar{\theta}}{\partial x'_j}+\bar{u}_j\frac{\partial\delta\bar{\theta}}{\partial x_j}=\kappa\frac{\partial^2\delta\bar{\theta}}{\partial x'_j\partial x'_j}+\kappa\frac{\partial^2\delta\bar{\theta}}{\partial x_j\partial x_j}+\frac{\partial\tau'_{\theta j}}{\partial x'_j}-\frac{\partial\tau_{\theta j}}{\partial x_j}. \tag{6}$$

Multiplying the above equation with $2\delta\bar{\theta}$, then we have

$$\begin{aligned}&\frac{\partial(\delta\bar{\theta})^2}{\partial t}+\frac{\partial}{\partial x'_j}[\bar{u}'_j(\delta\bar{\theta})^2]+\frac{\partial}{\partial x_j}[\bar{u}_j(\delta\bar{\theta})^2]\\&\quad=\kappa\frac{\partial^2(\delta\bar{\theta})^2}{\partial x'_j\partial x'_j}+\kappa\frac{\partial^2(\delta\bar{\theta})^2}{\partial x_j\partial x_j}-2\kappa\left(\frac{\partial\delta\bar{\theta}}{\partial x'_j}\right)^2-2\kappa\left(\frac{\partial\delta\bar{\theta}}{\partial x_j}\right)^2\\&\qquad+2\frac{\partial\delta\bar{\theta}\tau'_{\theta j}}{\partial x'_j}-2\frac{\partial\delta\bar{\theta}\tau_{\theta j}}{\partial x_j}-2\tau'_{\theta j}\frac{\partial\delta\bar{\theta}}{\partial x'_j}+2\tau_{\theta j}\frac{\partial\delta\bar{\theta}}{\partial x_j}.\end{aligned} \tag{7}$$

Define the distance between $\mathbf{x}'$ and $\mathbf{x}$ as $\mathbf{r}=\mathbf{x}'-\mathbf{x}$, and when $|\mathbf{r}|\to 0$, the turbulence can be assumed as locally homogeneous. Taking average on the above equation and considering the relation $\partial/\partial r_j=\partial/\partial x'_j=-\partial/\partial x_j$, we can get

$$\begin{aligned}&\frac{\partial\langle(\delta\bar{\theta})^2\rangle}{\partial t}+\frac{\partial}{\partial r_j}[\langle\bar{u}'_j(\delta\bar{\theta})^2\rangle-\langle\bar{u}_j(\delta\bar{\theta})^2\rangle]\\&\quad=2\kappa\frac{\partial^2\langle(\delta\bar{\theta})^2\rangle}{\partial r_j\partial r_j}-2\kappa\left\langle\left(\frac{\partial\delta\bar{\theta}}{\partial x'_j}\right)^2\right\rangle-2\kappa\left\langle\left(\frac{\partial\delta\bar{\theta}}{\partial x_j}\right)^2\right\rangle\\&\qquad+2\frac{\partial}{\partial r_j}[\langle\delta\bar{\theta}\tau'_{\theta j}\rangle+\langle\delta\bar{\theta}\tau_{\theta j}\rangle]-2\left\langle\tau'_{\theta j}\frac{\partial\delta\bar{\theta}}{\partial x'_j}\right\rangle+2\left\langle\tau_{\theta j}\frac{\partial\delta\bar{\theta}}{\partial x_j}\right\rangle\end{aligned} \tag{8}$$

In the above equation, the $\langle\rangle$ stands for the ensemble average in general, and can simply be the spatial average in the local homogeneous directions instead. In a simplified form, the above equation can be written as

$$\frac{\partial D_{\theta\theta}}{\partial t}+\frac{\partial D_{j\theta\theta}}{\partial r_j}=2\kappa\frac{\partial^2 D_{\theta\theta}}{\partial r_j\partial r_j}-\varepsilon_\theta-\varepsilon^f_\theta+T_\theta. \tag{9}$$

Hence, we get the dynamical equation for the structure function of the resolved-scale scalar fluctuation, it is the generalized form of Yaglom equation for LES. Here

$$D_{\theta\theta}(\mathbf{r})=\langle[\bar{\theta}(\mathbf{x}+\mathbf{r})-\bar{\theta}(\mathbf{x})]^2\rangle \tag{10}$$

is the second order structure function of $\bar{\theta}$, and

$$D_{j\theta\theta}(\mathbf{r})=\langle[\bar{u}_j(\mathbf{x}+\mathbf{r})-\bar{u}_j(\mathbf{x})][\bar{\theta}(\mathbf{x}+\mathbf{r})-\bar{\theta}(\mathbf{x})]^2\rangle \tag{11}$$

is the third order structure function of $\bar{u}_j$ and $\bar{\theta}$. ε_θ and ε^f_θ represent the molecular and the turbulent dissipation rate of scalar variance, and under the local homogeneity assumption, they become

$$\varepsilon_\theta=2\kappa\left\langle\left(\frac{\partial\delta\bar{\theta}}{\partial x'_j}\right)^2+\left(\frac{\partial\delta\bar{\theta}}{\partial x_j}\right)^2\right\rangle=4\kappa\left\langle\left(\frac{\partial\bar{\theta}}{\partial x_j}\right)^2\right\rangle, \tag{12}$$

and

$$\varepsilon_\theta^f = 2\left\langle \tau'_{\theta j}\frac{\partial \delta\bar{\theta}}{\partial x'_j} - \tau_{\theta j}\frac{\partial \delta\bar{\theta}}{\partial x_j}\right\rangle = 4\left\langle \tau_{\theta j}\frac{\partial \bar{\theta}}{\partial x_j}\right\rangle. \tag{13}$$

The scalar transport between resolved scale and the unresolved subgrid scale is represented by T_θ,

$$T_\theta = 2\frac{\partial}{\partial r_j}\langle(\tau_{\theta j}+\tau'_{\theta j})\delta\bar{\theta}\rangle. \tag{14}$$

2.2. New subgrid eddy diffusivity model

If the subgrid scalar flux is assumed to follow the eddy diffusivity hypothesis

$$\tau_{\theta j} = \kappa_t\frac{\partial\bar{\theta}}{\partial x_j}, \tag{15}$$

and κ_t is further assumed to be constant in the local homogeneous directions, then the turbulent dissipation becomes

$$\varepsilon_\theta^f = 4\kappa_t\left\langle\left(\frac{\partial\bar{\theta}}{\partial x_j}\right)^2\right\rangle, \tag{16}$$

and the transport term becomes

$$\begin{aligned} T_\theta &= 2\kappa_t\frac{\partial}{\partial r_j}\left\langle\left(\frac{\partial\bar{\theta}'}{\partial x'_j}+\frac{\partial\bar{\theta}}{\partial x_j}\right)\delta\bar{\theta}\right\rangle \\ &= 2\kappa_t\frac{\partial}{\partial r_j}\left\langle\left(\frac{\partial\delta\bar{\theta}}{\partial x'_j}-\frac{\partial\delta\bar{\theta}}{\partial x_j}\right)\delta\bar{\theta}\right\rangle = 2\kappa_t\frac{\partial^2 D_{\theta\theta}}{\partial r_j\partial r_j}. \end{aligned} \tag{17}$$

Substitute Eqs. (12), (16) and (17) into Eq. (9), we can get

$$\frac{\partial D_{\theta\theta}}{\partial t}+\frac{\partial D_{j\theta\theta}}{\partial r_j} = 2(\kappa+\kappa_t)\frac{\partial^2 D_{\theta\theta}}{\partial r_j\partial r_j} - 4(\kappa+\kappa_t)\left\langle\left(\frac{\partial\bar{\theta}}{\partial x_j}\right)^2\right\rangle. \tag{18}$$

Neglecting the time-dependent term $\partial D_{\theta\theta}/\partial t$, the eddy diffusivity coefficient can be obtained from Eq. (18),

$$\kappa+\kappa_t = \frac{\frac{\partial D_{j\theta\theta}}{\partial r_j}}{2\frac{\partial^2 D_{\theta\theta}}{\partial r_j\partial r_j} - 4\left\langle\left(\frac{\partial\bar{\theta}}{\partial x_j}\right)^2\right\rangle}. \tag{19}$$

At high Peclet number, the scalar turbulence can be further assumed locally isotropic, and the molecular diffusivity κ is negligible compared with the eddy diffusivity κ_t. In this case, $D_{\theta\theta}(\mathbf{r})$ is a scalar function, and $D_{j\theta\theta}(\mathbf{r})$ is a vector function, and they have the following form

$$D_{\theta\theta}(\mathbf{r}) = D_{\theta\theta}(r^2), \quad D_{j\theta\theta}(\mathbf{r}) = D_{l\theta\theta}(r^2)\frac{r_j}{r}. \tag{20}$$

In the above equation, $D_{l\theta\theta}$ is the longitudinal mixed structure function defined as $D_{l\theta\theta} = \langle[\bar{u}(\mathbf{x}+\mathbf{r})-\bar{u}(\mathbf{x})][\bar{\theta}(\mathbf{x}+\mathbf{r})-\bar{\theta}(\mathbf{x})]^2\rangle$, in which $\bar{u}$ is the velocity component along $\mathbf{r}$ direction. According to Eq. (20), we have

$$\frac{\partial^2 D_{\theta\theta}}{\partial r_j\partial r_j} = \left(\frac{\partial^2}{\partial r^2}+\frac{2}{r}\frac{\partial}{\partial r}\right)D_{\theta\theta} = \frac{1}{r^2}\frac{\partial}{\partial r}\left(r^2\frac{\partial D_{\theta\theta}}{\partial r}\right), \tag{21}$$

and

$$\frac{\partial D_{j\theta\theta}}{\partial r_j} = \left(\frac{\partial}{\partial r}+\frac{2}{r}\right)D_{l\theta\theta} = \frac{1}{r^2}\frac{\partial}{\partial r}(r^2 D_{l\theta\theta}). \tag{22}$$

Substitute the above expressions into Eq. (18), and neglect the molecular diffusivity κ and the time-dependent term, we can get

$$\frac{\partial}{\partial r}(r^2 D_{l\theta\theta}) = 2\kappa_t\frac{\partial}{\partial r}\left(r^2\frac{\partial D_{\theta\theta}}{\partial r}\right) - 4\kappa_t\left\langle\left(\frac{\partial\bar{\theta}}{\partial x_j}\right)^2\right\rangle r^2. \tag{23}$$

Integrate the above equation from 0 to r, it can be obtained that

$$D_{l\theta\theta} = 2\kappa_t\frac{\partial D_{\theta\theta}}{\partial r} - \frac{4}{3}\kappa_t\left\langle\left(\frac{\partial\bar{\theta}}{\partial x_j}\right)^2\right\rangle r, \tag{24}$$

and the eddy diffusivity can be obtained finally

$$\kappa_t = \frac{-3D_{l\theta\theta}}{4\left\langle\frac{\partial\bar{\theta}}{\partial x_j}\frac{\partial\bar{\theta}}{\partial x_j}\right\rangle r - 6\frac{\partial D_{\theta\theta}}{\partial r}}. \tag{25}$$

In Eq. (25), κ_t appears to be a function of r. In the practical application of this model in the simulation of scalar turbulence, r is taken to be equal to the filter width. Hence Eq. (25) describes the relationship between SGS eddy diffusivity and the filter width, and in this way the model is compatible with the rest of the large-eddy simulation equations.

3. Large eddy simulation of scalar turbulence with the new subgrid eddy diffusivity model

The new subgrid eddy diffusivity model has been applied to the large eddy simulation of scalar transport in decaying isotropic turbulence and fully developed turbulent channel flow. The velocity field is governed by the filtered incompressible Navier–Stokes equation,

$$\frac{\partial\bar{u}_i}{\partial t}+\bar{u}_j\frac{\partial\bar{u}_i}{\partial x_j} = -\frac{1}{\rho}\frac{\partial\bar{p}}{\partial x_i}+\nu\frac{\partial^2\bar{u}_i}{\partial x_j\partial x_j}+\frac{\partial\tau_{ij}}{\partial x_j}, \tag{26}$$

$$\frac{\partial\bar{u}_i}{\partial x_i} = 0, \tag{27}$$

where $\tau_{ij} = -(\overline{u_i u_j}-\bar{u}_i\bar{u}_j)$ is the subgrid scale stress and can be modelled by the SGS eddy viscosity model

$$\tau_{ij} = 2\nu_t\bar{s}_{ij}+\frac{1}{3}\tau_{kk}\delta_{ij}, \tag{28}$$

where $\bar{s}_{ij} = (\partial\bar{u}_i/\partial x_j+\partial\bar{u}_j/\partial x_i)/2$ is the strain rate tensor of the resolved velocity field. The SGS eddy viscosity coefficient ν_t is predicted by the model recently proposed by Cui et al. (2004), which is derived from the modified Kolmogorov equation

$$\nu_t = \frac{-5D_{lll}}{8\langle\bar{s}_{ij}\bar{s}_{ij}\rangle r - 30\frac{\partial D_{ll}}{\partial r}}, \tag{29}$$

where $D_{ll} = \langle[\bar{u}(x+r)-\bar{u}(x)]^2\rangle$ and $D_{lll} = \langle[\bar{u}(x+r)-\bar{u}(x)]^3\rangle$ are the second and third order longitudinal structure functions.

3.1. Decaying isotropic turbulence

The scalar transport in a decaying isotropic turbulence is first simulated by large eddy simulation employing the SGS eddy diffusivity model derived above along with the SGS eddy viscosity model by Cui et al. (2004), and compared with the experimental results by Warhaft (1984).

Eqs. (26), (27) and (1) are solved by spectral method employing Fourier series in a cubic computational domain with periodic conditions in all the three directions. The aliasing error is removed by spectral truncation method (also referred to as 3/2-rule). See Cui et al. (2000) for more details. The decaying isotropic turbulence is initialized by the velocity field obtained by direct numerical simulation at $Re_\lambda = 160$. The large eddy simulation is performed on 32^3 grids. The velocity field is allowed to adjust for one turn-over time, and then the isotropic scalar field with Gaussian distribution is introduced at the molecular Prandtl number $Pr = \nu/\kappa = 1.0$.

The time history of turbulent kinetic energy $E = \langle \bar{u}_i \bar{u}_i \rangle / 2$ is shown in Fig. 1. From this figure, the decay exponent of turbulent kinetic energy can be estimated as 1.4 which is in agreement with the values reported in literature (between 1.15 and 1.45). Fig. 2 shows the time history of the scalar variance $E_\theta = \langle \bar{\theta}^2 \rangle / 2$ obtained by large eddy simulation with the new eddy diffusivity model. The decay exponent estimated from this figure is 2.89. In Warhaft's experiment, the measured decay exponent is between 2.8 and 3.2, corresponding to the different distances from scalar source to the grid at the entrance of the wind tunnel.

3.2. Turbulent channel flow

The new eddy diffusivity model is further applied to the large eddy simulation of a turbulent channel flow with uniform heat flux at the walls, and compared with the direct numerical simulation (DNS) by Kawamura et al. (2000).

As is shown in Fig. 3, the flow driven by a constant mean pressure gradient in streamwise direction (x) is confined between two parallel walls, which are uniformly

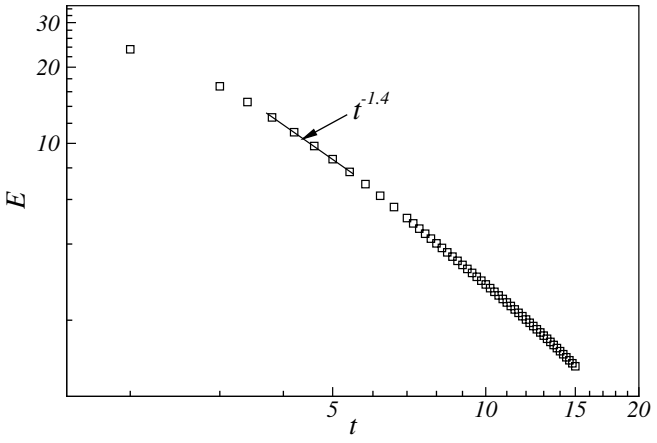

Fig. 1. Time history of turbulent kinetic energy.

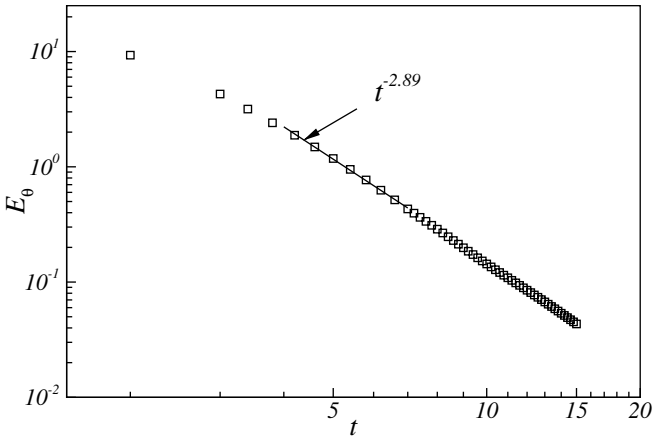

Fig. 2. Time history of scalar variance.

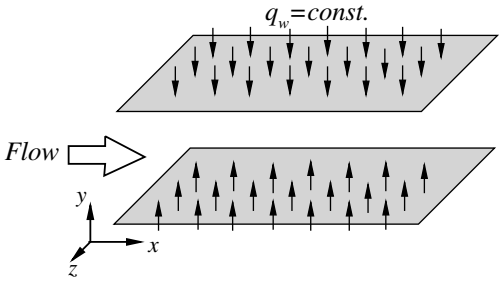

Fig. 3. Computation domain and boundary conditions.

heated. The buoyancy effect is not taken into consideration in this case, and the temperature T is treated as passive scalar in our simulation. The uniform heat flux at the walls cause the statistically averaged temperature increase linearly with respect to x, hence we can decompose T as

$$T = Gx + \theta, \tag{30}$$

and the filtered equation for $\bar{\theta}$ becomes

$$\frac{\partial \bar{\theta}}{\partial t} + \bar{u}_j \frac{\partial \bar{\theta}}{\partial x_j} = \kappa \frac{\partial^2 \bar{\theta}}{\partial x_j \partial x_j} + \frac{\partial \tau_{\theta j}}{\partial x_j} - G\bar{u}_1. \tag{31}$$

For more details concerning the constant G, see Kawamura et al. (2000).

To evaluate the performance of the newly proposed model, the large-eddy simulation Eqs. (26), (27) and (31) are solved together with three different SGS eddy viscosity and eddy diffusivity models:

1. The eddy viscosity ν_t and diffusivity κ_t are given by the new models (NM) as are shown in Eqs. (29) and (25), respectively. In turbulent channel flow with uniformly heated walls, turbulence is homogeneous in streamwise (x) and spanwise (z) directions, and hence the average in Eq. (29) and (25) is taken over these two directions. The inhomogeneous effect in the wall-normal (y) direction is considered by assuming that ν_t and κ_t are functions of y. Approaching the wall, $D_{l0\theta}$ goes to zero as

y^3 and $\langle(\partial\bar{\theta}/\partial x_j)^2\rangle$ in Eq. (25) is finite, and hence κ_t approaches zero as y^3 when $y \to 0$. This is in consistent with the wall limiting behavior of the scalar flux $\tau_{\theta 2} = \overline{v\theta} - \bar{v}\bar{\theta}$. The basic assumption of the model is local isotropy. For simplicity, $\mathbf{r}$ is taken along x direction, and $|\mathbf{r}| = \Delta_x$. The longitudinal velocity structure function D_{ll} and D_{lll} in Eq. (29), and the mixed structure function $D_{l\theta\theta}$ in Eq. (25) are calculated by the streamwise velocity component u'.

2. v_t is given by the standard Smagorinsky model (SM) and κ_t is obtained from v_t by $\kappa_t = v_t/Pr_t$, where Pr_t is the SGS turbulence Prandtl number, and takes the standard value of 0.7 in present study.
3. v_t is given by the dynamical Smagorinsky model (DM) and $\kappa_t = v_t/Pr_t$ with $Pr_t = 0.7$.

The governing equations are spatially discretized by spectral method and temporally advanced by third order time-splitting method. In streamwise and spanwise directions, periodic conditions are imposed on $\bar{u}_i$ and $\bar{\theta}$, and Fourier–Galerkin method is adopted in these two homogeneous directions. At the walls, no-slip conditions are adopted for velocity. By employing the decomposition (30), the wall condition for temperature becomes $\bar{\theta} = 0$. Hence Chebyshev-collocation method is employed in wall-normal direction. The aliasing error is removed by spectral truncation method. For more details, see Xu et al. (1996).

In present simulation, the flow rate is kept constant, and the Reynolds number based on the bulk mean velocity U_m and channel half width H is fixed at 7000. The molecular Prandtl number takes the value of 0.7. The computational domain extends $2\pi H \times 2H \times \pi H$ in streamwise, wall normal and spanwise directions with $64 \times 65 \times 64$ grids, respectively. The calculation is carried out until the flow becomes statistically steady, and continued for about $100H/U_m$ to obtain enough samples for turbulence statistics. The statistical results are compared with the DNS results of Moser et al. (1999) (denoted by MKM in the figures) and Kawamura et al. (2000). It is worth to note that the DNS results shown in the following figures are unfiltered. We have checked the SGS contribution to the total turbulent kinetic energy by truncating the DNS data ($Re = 7000$ with the resolution of $256 \times 192 \times 256$) to the LES resolution used in present study, and it is found that the SGS motion contribute about 5% to the total turbulent kinetic energy. Hence in the following assessment of the SGS models, the influence of the filtered SGS motion to the turbulence statistics is neglected.

Fig. 4 shows the mean velocity profile computed with the three different SGS models and compared with the DNS results obtained by Moser et al. (1999). It can be seen that the mean velocity distribution predicted by the new model and the dynamical model agrees very well with the DNS result, while the Smagorinsky model has a poorer performance. The distributions of turbulence intensities and Reynolds shear stress obtained by present large eddy simulations are shown in Fig. 5. In streamwise direction, the turbulence intensity predicted by the new model and the dynamical model are both in good agreement with the DNS results, while the Smagorinsky model gives an overshoot prediction. In wall-normal direction, all the three models underestimate the turbulence intensity, but in the near-wall region, the behavior of the new model and the dynamical model is much better than the Smagorinsky model. For spanwise turbulence intensity, the peak value and peak position given by the new model and the dynamical model are much better than the Smagorinsky model. For the distribution of Reynolds shear stress, the three models have similar accuracy, and the new model and the dynamical model yield slightly better result than the Smagorinsky model near the center of the channel.

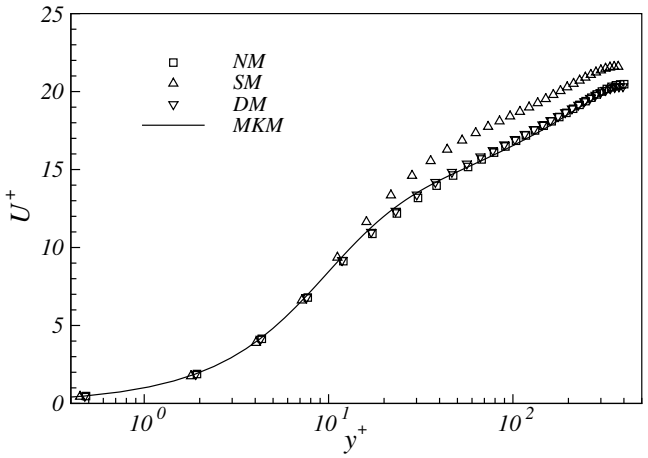

Fig. 4. Mean velocity profile.

Fig. 6 shows the mean temperature profile in comparison with the DNS result by Kawamura et al. (2000). The results given by the new model and the dynamical model are in good agreement with the DNS result. Fig. 7 shows the distribution of the intensity of temperature fluctuation. Among the three models, the result given by the new model agrees best with the DNS result. Near the wall, the Smagorinsky model over predicts the temperature fluctuation, while the dynamical model underestimates the level of temperature fluctuation. Away from the wall, the result obtained by the new model is closest to the DNS result than those by the other two models. The distributions of temperature flux in streamwise and wall-normal directions are shown in Fig. 8(a) and (b), respectively. For streamwise temperature flux, the peak value and the peak position predicted by the new model and the dynamical model agree well with the DNS result and are much better than that given by the Smagorinsky model. In the wall-normal direction, the temperature flux is underestimated by all the three models near the peak position, and near the center of the channel, the behavior of the new model and the dynamical model is slightly better than the Smagorinsky model.

To evaluate the new model in the sense of computational cost, the CPU time consumed per time step by the

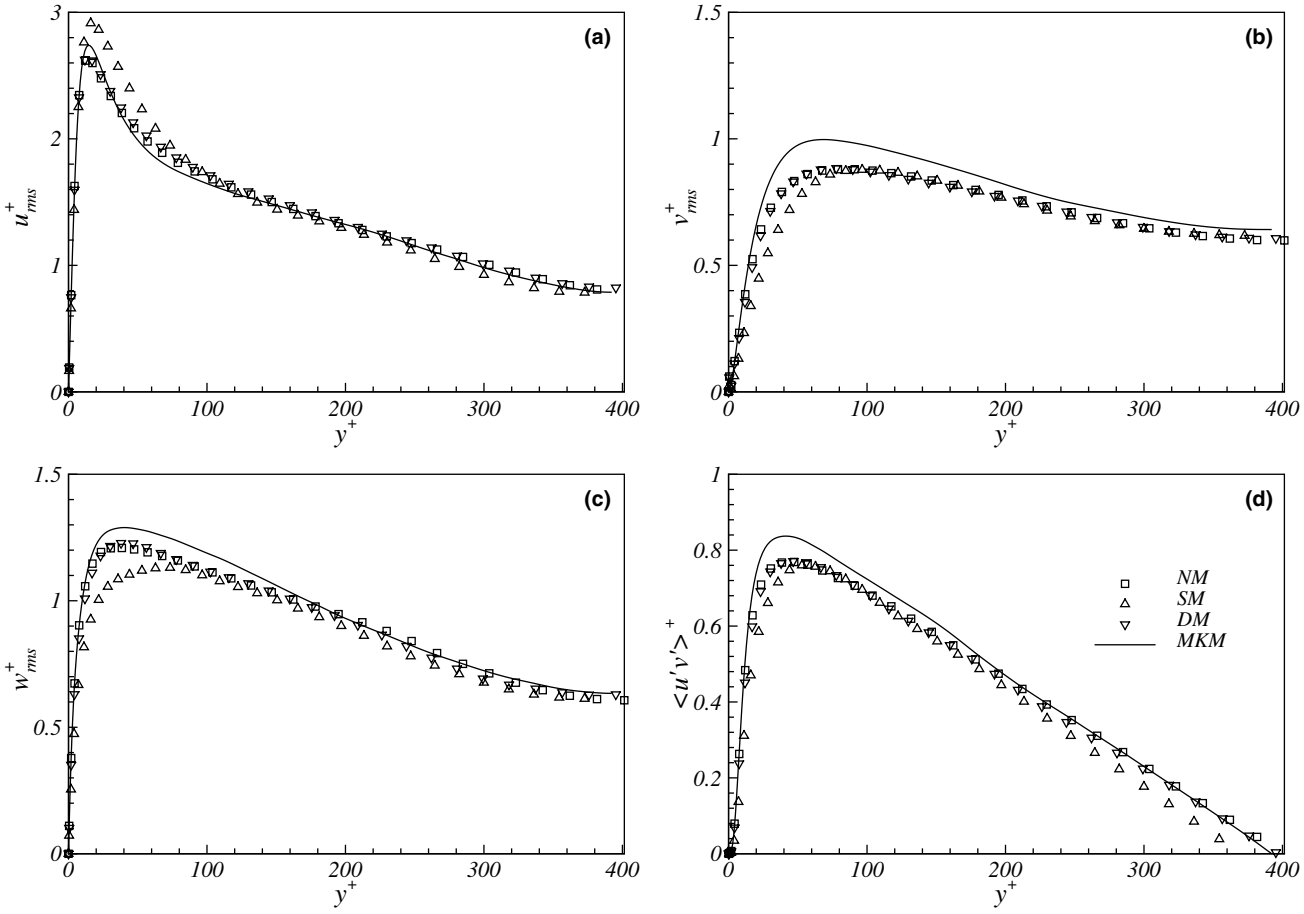

Fig. 5. Distribution of (a) u^+_{rms}, (b) v^+_{rms}, (c) w^+_{rms} and (d) $\langle u'v' \rangle^+$.

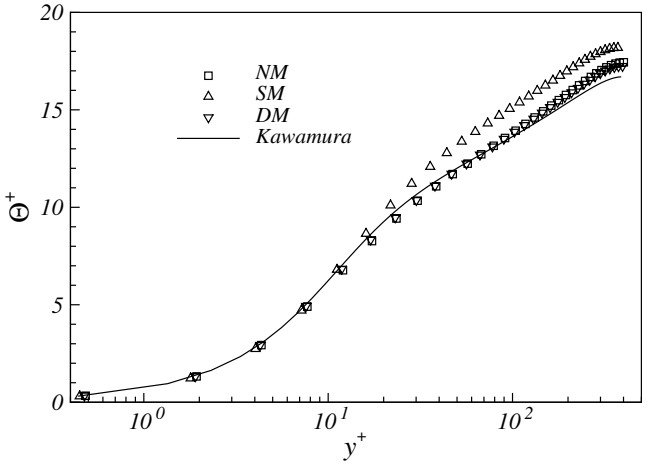

Fig. 6. Mean scalar profile.

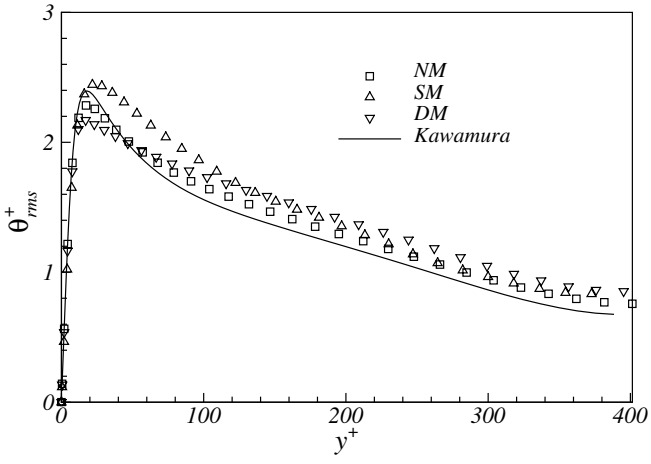

Fig. 7. Distribution of the intensity of scalar fluctuation.

computations employing SM, DM and NM is shown in Table 1. The CPU time consumed by using dynamical Smagorinsky model is 1.53 times that by standard Smagorinsky model. The ratio of the CPU time by the new model to that by the standard Smagorinsky model is 1.23. This suggests that compared to the dynamical model, nearly 20% computational costs can be saved in terms of CPU time by using the new model without any loss in accuracy.

4. Conclusions

In present paper, a new subgrid eddy diffusivity model is used for large eddy simulation of scalar turbulence. This

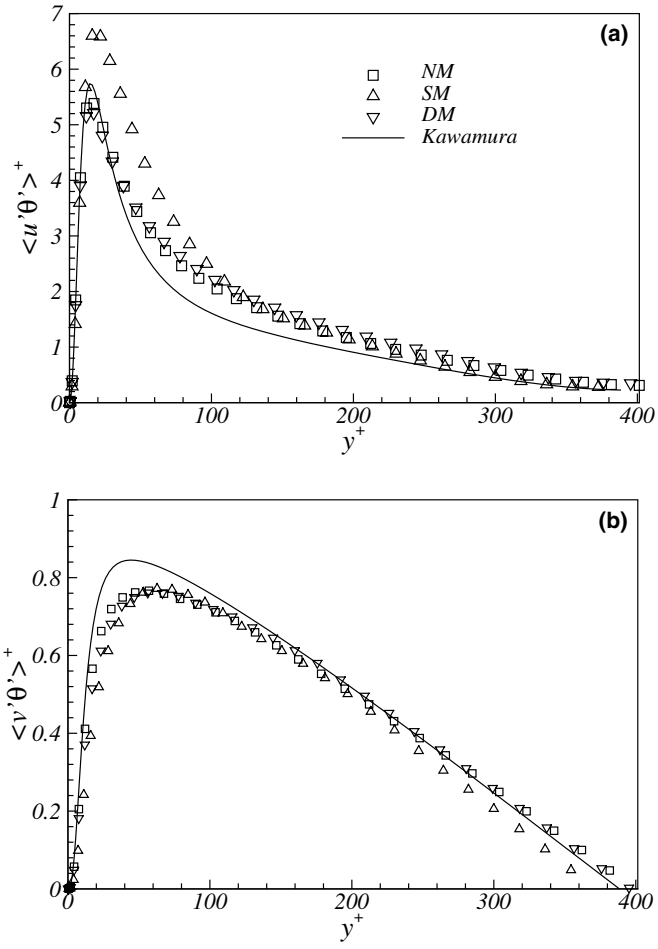

Fig. 8. Distribution of scalar flux in (a) streamwise and (b) wall-normal direction.

Table 1
Comparison of computational costs

	SM	DM	NM
CPU time per step (s)	9.42	14.4	11.6
Ratio	1.0	1.53	1.23

new model is based on the modified Yaglom equation for scalar fluctuation at resolved scale, which is believed to be able to describe the scalar transport between the resolved grid scale and the unresolved subgrid scale exactly. The new model is evaluated by the application in the large eddy simulation of scalar transport in the decaying isotropic turbulence and the fully developed turbulent channel flow. In isotropic turbulence, the decaying exponent of the scalar variance is in agreement with the wind tunnel measurement conducted by Warhaft (1984). The standard Smagorinsky model and dynamical Smagorinsky model are also adopted as well as the new model in the large eddy simulation of turbulent channel flow with uniform scalar flux at the wall. By the comparison of the first and second order turbulent statistics with the DNS results by Kawamura et al. (2000), it is shown that the new model can achieve the similar accuracy as that by the dynamical model, while the computational cost in terms of CPU time can be saved nearly 20% by the new model rather than by the dynamical model.

In the practical application of the new subgrid eddy diffusivity model, the computation of the structure function is somewhat more complicated than other models, which will be further simplified in our future work. The model will also be tested in more complex turbulent flows, such as the flow with separation and unsteadiness.

Acknowledgements

The authors wish to express their sincere gratitude to National Natural Science Foundation of China (Grant No. 10272065 and 10472053) and Sino-French Laboratory (LIAMA).

References

Bogucki, D., Domaradzki, J.A., Yeung, P.K., 1997. Direct numerical simulations of passive scalars with $Pr > 1$ advected by turbulent flow. J. Fluid Mech. 343, 111–130.

Cui, G.X., Chen, Y.G., Zhang, Z.S., Xu, C.X., 2000. Transportation of passive scalar in inhomogeneous turbulence. Acta Mech. Sinica (English Series) 16 (1), 21–28.

Cui, G.X., Zhou, H.B., Zhang, Z.S., Shao, L., 2004. A new dynamic subgrid eddy viscosity model with application to turbulent channel flow. Phys. Fluids 16 (8), 2835–2842.

Kawamura, H., Abe, H., Shingai, K., 2000. DNS of turbulence and heat transport in a channel flow with different Reynolds and Prandtl numbers and boundary conditions. In: Proceeding of the third international symposium on turbulence, heat and mass transfer, Nagoya, Japan, 15–32.

Lesieur, M., Rogallo, R., 1989. Large-eddy simulation of passive scalar diffusion in isotropic turbulence. Phys. Fluids A 1, 718–722.

Moser, R.D., Kim, J., Mansour, N.N., 1999. Direct numerical simulation of turbulent channel flow up to $Re_\tau = 590$. Phys. Fluids 11, 943–945.

Mydlarski, L., Warhaft, Z., 1998. Passive scalar statistics in high-Peclet-number grid turbulence. J. Fluid Mech. 358, 135–175.

Warhaft, Z., 1984. The interference of thermal fields from line sources in grid turbulence. J. Fluid Mech. 144, 363–387.

Xu, C.X., Zhang, Z., den Toonder, J.M.J., Nieuwstadt, F.T.M., 1996. Origin of high kurtosis levels in the viscous sublayer. Direct numerical simulation and experiments. Phys. Fluids 8 (7), 1938–1944.

Zhou, H.B., Cui, G.X., Zhang, Z.S., 2002. Dependence of turbulent scalar flux on molecular Prandtl number. Phys. Fluids 14 (7), 2388–2394.